

Papers published in *Hydrology and Earth System Sciences Discussions* are under open-access review for the journal *Hydrology and Earth System Sciences*

Tibet land modeling

K. Yang et al.

Some practical notes on the land surface modeling in the Tibetan Plateau

K. Yang, Y.-Y. Chen, and J. Qin

Laboratory of Tibetan Environment Changes and Land Surface Processes, Institute of Tibetan Plateau Research, Chinese Academy of Sciences, Beijing 100085, China

Received: 21 January 2009 – Accepted: 2 February 2009 – Published: 27 February 2009

Correspondence to: K. Yang (yangk@itpcas.ac.cn)

Published by Copernicus Publications on behalf of the European Geosciences Union.

Title Page

Abstract

Introduction

Conclusions

References

Tables

Figures



Back

Close

Full Screen / Esc

Printer-friendly Version

Interactive Discussion



Abstract

The Tibetan Plateau is a key region of land-atmosphere interactions, as it provides an elevated heat source to the middle-troposphere. The Plateau surfaces are typically characterized by alpine meadows and grasslands in the central and eastern part while by alpine deserts in the western part. This study evaluates performance of three state-of-the-art land surface models (LSMs) for the Plateau typical land surfaces. The LSMs of interest are SiB2 (the Simple Biosphere), CoLM (Common Land Model), and Noah. They are run with default parameters at typical alpine meadow sites in the central Plateau and typical alpine desert sites in the western Plateau.

The recognized key processes and modeling issues are as follows. First, soil stratification is a typical phenomenon beneath the alpine meadows, with dense roots and soil organic matters within the topsoil, and it controls the profile of soil moisture in the central and eastern Plateau; all models significantly under-estimate the soil moisture within the topsoil. Second, a soil surface resistance controls the surface evaporation from the alpine deserts but it has not been reasonably modeled in LSMs; a new scheme is proposed to determine this resistance from soil water content. Third, an excess resistance controls sensible heat fluxes from dry bare-soil or sparsely vegetated surfaces, and all LSMs significantly under-predict the ground-air temperature difference in the daytime. A parameterization scheme for this resistance has been shown effective to remove this bias.

1 Introduction

The Tibetan Plateau (TP) is one of regions with strong land-atmosphere interactions, due to strong solar heating over the Plateau. TP land processes are generally characterized by three features. The first is apparent diurnal variations due to strong solar radiation and low air density. The solar irradiance over the Plateau was frequently observed exceeding 1200 W m^{-2} near noon, which results in very strong diurnal change

HESSD

6, 1291–1320, 2009

Tibet land modeling

K. Yang et al.

Title Page

Abstract

Introduction

Conclusions

References

Tables

Figures

◀

▶

◀

▶

Back

Close

Full Screen / Esc

Printer-friendly Version

Interactive Discussion



Tibet land modeling

K. Yang et al.

Title Page

Abstract

Introduction

Conclusions

References

Tables

Figures



Back

Close

Full Screen / Esc

Printer-friendly Version

Interactive Discussion



of the surface energy budget and near-surface meteorological variables. For instance, the diurnal range of the surface skin temperature can exceed 60 K. The second is the distinct seasonal march of the surface water and energy budget in the central and eastern TP. Before the onset of the monsoon (about the end of May to the middle of June), the surface is very dry and the sensible heat flux dominates the surface energy budget; after the onset, the land surface becomes wet due to frequent rainfall events and it is the latent heat flux that dominates the energy budget until the withdraw of the monsoon in September. The third is the contrast between the dry western region and the wet eastern region. Annual precipitation amount is about 400 mm or more in most of central and eastern TP (CE-TP), while it is around 100 mm or less in the western TP (W-TP). Under the unique Plateau climate, the land surfaces are typically characterized by alpine meadows and grasslands in CE-TP while by alpine deserts in W-TP.

It has been widely accepted that TP provides an elevated, huge heat source to the middle-troposphere and the land-atmosphere interactions play an important role in the formation of the Asian monsoon (Ye and Gao, 1979; Yanai et al., 1992; Yanai and Wu, 2006). However, these interactions are not well represented in current models. Figure 1 shows the surface energy budget on a central Plateau area (near Naqu city) in four numerical weather prediction models: ECPC (Experimental Climate Prediction Center, at the Scripps Institution of Oceanography), JMA (Japan Meteorological Agency), NCEP (National Centers for Environmental Prediction, USA), and UKMO (Met Office, UK). The data are provided by the CEOP (Coordinated Enhanced Observing Period) centralized data archive system (Nemoto et al., 2007). See Yang et al. (2007) for a brief description of the models. Figure 1 shows that the surface energy budgets are quite discrepant among the four models from the pre-monsoon period (before DOY 151) to the monsoon period (after DOY 151), 2003. ECPC and NCEP yield an unexpected seasonal march of the energy budget, while JMA and UKMO shows a too weak seasonal march of the latent heat flux, comparing to observations in 1998 (not shown). Large uncertainties in the Bowen Ratio were also found in an inter-comparison of offline land surface models (LSMs) by Takayabu et al. (2001). One of possible reasons

is that the land processes in this region have not been well represented in the models.

Since 1998, several field experiments have been or are being implemented in this region, including the GEWEX (Global Energy and Water cycle Experiment) Asian Monsoon Experiment-Tibet (GAME-Tibet; Koike et al., 1999), the Tibetan Plateau Experiment of Atmospheric Sciences (TIPEX; Xu et al., 2002), the CEOP Asia–Australia Monsoon Project in Tibet (CAMP-Tibet; Koike, 2004), the China and Japan intergovernmental weather disaster program (JICA) (Xu et al., 2008), and the Tibetan Observation and Research Platform (TORP; Ma et al., 2008). Their overall goal is to understand the Plateau energy and water cycle and clarifies its role in the Asian monsoon system. Undoubtedly, these experiments have advanced our understanding to land processes in this region (Ma et al., 2002; Tanaka et al., 2003; Yang et al., 2005; Hu et al., 2006; Li and Sun, 2008). However, these achievements have not been integrated into state-of-the-art LSMs, and therefore, there is a big gap between these experimental studies and the LSM development.

This study evaluates the modeling ability of three widely used LSMs against experimental data for the Plateau land surfaces, and then identifies key processes and modeling issues. The land surface modeling is conducted at two types of sites, representing the typical alpine meadows in CE-TP and the typical alpine deserts in W-TP, respectively. Though these LSMs are run with default parameters, due to lack of true values of model parameters, we believe the results presented in this paper are robust.

2 Observations and models

In situ data were collected through the GAME-Tibet during an intensive observing period (IOP, May~September, 1998). Figure 2 shows the observing network. To achieve a better representativeness to the entire Plateau, the observational sites were deployed along a north-south transect and a west-east transect; more than half of them were placed within a meso-scale area (30.5–33 N, 91–92.5 E). All sites were above 4000 m a.s.l.

Tibet land modeling

K. Yang et al.

Title Page

Abstract

Introduction

Conclusions

References

Tables

Figures

◀

▶

◀

▶

Back

Close

Full Screen / Esc

Printer-friendly Version

Interactive Discussion



Tibet land modeling

K. Yang et al.

Title Page

Abstract

Introduction

Conclusions

References

Tables

Figures



Back

Close

Full Screen / Esc

Printer-friendly Version

Interactive Discussion



The simulations were conducted at two alpine meadow sites (Anduo or Amdo, MS3478) in CE-TP and at two alpine desert sites (Shiquanhe or SQH, Gerze) in W-TP. CE-TP is typically affected by the monsoon while W-TP by the westerly, and therefore, their climatology is very different and the land conditions are also different. At the alpine meadow sites, the surfaces are nearly bare-soil in the pre-monsoon season (it was before 15 June in 1998) but turn to grassland afterwards; measurements during GAME-Tibet included surface skin temperature, soil moisture profile, and surface turbulent fluxes from May to September 1998. The surface skin temperature was converted from downward and upward longwave radiation with the surface emissivity given by the observers, soil moisture was measured by TDR, and turbulence fluxes by eddy-covariance system. At the alpine desert sites, the surface was nearly bare soil, and measurements included surface skin temperature, soil moisture at 0–15 cm, while turbulent fluxes were not available. The surface temperature was directly measured using a thermometer, with half of the sensor buried in the soil and half exposed to the air; the soil moisture was measured by TDR. The measuring period was also from May to September. Data averaged over each 30 or 60 min period was recorded.

The three models of interest are SiB2 (the Simple Biosphere scheme version 2; Sellers et al., 1996), Noah (Chen et al., 1996; Koren et al., 1999), and CoLM (Common Land Model; Dai et al., 2003). Table 1 shows their differences. (1) SiB2 uses three layers for solving soil moisture and the force restore method for solving soil skin temperature, while Noah and CoLM uses more layers to solve both soil moisture and soil temperature profiles. (2) SiB2 uses a K-theory aerodynamic model to solve the wind profile and heat/vapor transfer resistances within a canopy, while CoLM assumes wind speed within a canopy being equal to the frictional velocity above the canopy. Noah does not have such a canopy aerodynamic model. (3) SiB2 uses an empirical formula to estimate the soil surface resistance for evaporation, Noah also considers this resistance by using the relationship between evaporation efficiency and soil water content, but this resistance is neglected in the CoLM. (4) SiB2 updates canopy temperature by taking the heat storage of a canopy into account, while the canopy temperature in

Tibet land modeling

K. Yang et al.

CoLM is determined by the canopy radiation budget without considering the canopy heat storage. In Noah, land surfaces are divided into bare soil surface and vegetation surface, and each of them has a single surface temperature. (5) Both CoLM and Noah consider more processes, such as soil freezing/thawing and snow melting. Parameters for multiple soil horizons can be set in CoLM.

As soil and vegetation parameters are not available from observations, these models are run with individually specified default values of these parameters. Nevertheless, the analysis and conclusions presented in this study will not be much affected by this specification, though simulations would be much improved by tuning parameter values in the models.

In SiB2, soil parameters and vegetation parameters (classification and coverage) are derived from $1^\circ \times 1^\circ$ ISLSCP II (International Satellite Land Surface Climatology Project Initiative II) soil data (Global Soil Data Task, 2000) and vegetation data (Loveland et al., 2001). In Noah, the soil type is obtained from the FAO (Food and Agriculture Organization) data. The vegetation type is derived from UMD vegetation classification map (Hansen et al., 2000). In CoLM, land-water mask and land cover are derived from USGS vegetation data files. Soil types and parameters are merged from FAO and US general soil map (STATSGO) data. Both top soil layer (0–30 cm) and bottom soil layer (30–100 cm) data are provided. All soil and vegetation data are available at 30 arc resolution.

In addition, the parameterization of the transfer resistances in SiB2 canopy needs a set of aerodynamic parameters, which are calculated by a K-theory based model. For nearly bare-soil surfaces, LAI (Leaf Area Index) is very small, and the aerodynamic roughness length (z_{0m}) should approach the value for bare-soil surfaces. However, the K-theory in SiB2 produces the roughness length much less than this value, because this theory is not consistent with the classic mixing-length theory. On the other hand, Watanabe and Kondo (1990) developed a canopy model based on the mixing-length theory; it produces z_{0m} being spontaneously equal to the value for the bare-soil surface when LAI approaches zero. Considering small LAI values in the Plateau, we adopted

Title Page

Abstract

Introduction

Conclusions

References

Tables

Figures

◀

▶

◀

▶

Back

Close

Full Screen / Esc

Printer-friendly Version

Interactive Discussion



their canopy model to produce the aerodynamic parameters required in SiB2.

3 Model evaluations

3.1 At alpine meadows

The onset of the Plateau monsoon in 1998 was 15 June which was later than normal years. At Anduo site, the simulated period is from 11 May to 31 August. The amount of precipitation is only 7 mm during the dry season (or the pre-monsoon season) but reached 278 mm during the wet season (or the monsoon season). At MS3478, two model runs are conducted, respectively, for the dry period from 8 May to 17 June and for the wet period from 1 July to 16 September, due to data missing between the two periods. The amount of precipitation is 3 mm in the dry period and 318 mm in the wet period. Soil moisture and temperatures in all simulations are initialized with observed data.

The simulated results at the two alpine meadow sites are similar, and therefore, the following only introduces the results at Anduo site, as shown in Fig. 3 for the dry season and in Figure 4 for the wet season. To show clearly the comparisons between the observations and the simulations, only five-days are shown in each figure; the results for other days are not much different.

Figures 3a–4a show that the soil moisture near the surface (4 cm depth) is much under-estimated by all models for both seasons. This is related a special soil stratification under the Plateau meadows and will be discussed in Sect. 4.1.

Figures 3b–4b show the modeled surface temperature. The nighttime surface temperature is well simulated by CoLM. This may be attributed to both a reasonable specification of the soil thermal inertial and the well designed discrete scheme for soil thermal diffusion in CoLM. However, the daytime surface temperature is much under-estimated by all LSMs in the dry season. This is a severe modeling deficiency and will be addressed in Sect. 4.3.

Tibet land modeling

K. Yang et al.

Title Page

Abstract

Introduction

Conclusions

References

Tables

Figures

◀

▶

◀

▶

Back

Close

Full Screen / Esc

Printer-friendly Version

Interactive Discussion



Figure 3c shows that the sensible heat flux during the dry season is under-estimated by SiB2, but it is over-estimated by Noah and CoLM even though their daytime surface temperature is much under-estimated (see Fig. 3b). In the wet season, the sensible heat flux simulated by SiB2 looks better than by Noah and CoLM (Fig. 4c).

The discrepancies among the simulated latent heat fluxes are very large. For the dry season, Figure 3d shows that the latent heat flux is over-estimated by SiB2 while under-estimated by Noah. The latent heat flux in CoLM reaches the peak much earlier than the observed one in each day and then decreases rapidly. In the wet season, the observed latent heat flux is not credible due to an instrumental limitation, as indicated in Yang et al. (2004). Therefore, it is not easy to interpret the difference between the simulations and the observation. Nevertheless, it is clear that there are big discrepancies among the three models; particularly, CoLM produces much higher values than SiB2 and Noah do. This will be discussed in Sect. 4.2.

3.2 At alpine deserts

The western alpine meadow sites (SQH and Gerze) represent another typical surface related to the westerly-controlled condition. At SQH site, the simulated period is from May 1 to September 14, 1998, and the amount of precipitation is only 25 mm. At Gerze, the simulated period is much shorter (from 1 May to 15 June 1998) due to data missing afterwards, and there was not any precipitation event during this period. Therefore, both sites were very dry. The simulations are initialized with observed soil moisture and temperatures. As the models show similar performances at the two sites, the following only presents the results at SQH site.

Figure 5a shows the simulated surface temperature compared with the observations at SQH. Again, only a few days are shown and the results are typical throughout the simulated period. CoLM, again, clearly simulated better nighttime surface temperature than SiB2 and Noah do, but daytime surface temperature was much under-predicted by all models. This performance is similar to that for the alpine meadow sites in the dry season (Fig. 3b). This big error is not due to specifying a high soil thermal iner-

Title Page

Abstract Introduction

Conclusions References

Tables Figures

◀ ▶

◀ ▶

Back Close

Full Screen / Esc

Printer-friendly Version

Interactive Discussion



tial. Actually, the thermal conductivity is already close to its minimum value. e.g., it is about $0.3 \text{ W m}^{-2} \text{ K}^{-1}$ in SiB2. This modeling bias for dry surfaces will be investigated in Sect. 4.3.

Figure 5b shows the comparison of the liquid soil water between the observation (not available after DOY 211) and the simulations. CoLM and Noah simulated soil freezing and thawing processes and the figure only plots the liquid water content to compare with TDR-measured values. In general, all LSMs performed better for the desert sites than for the meadows sites. Nevertheless, the modeled biases are also clear. The soil moisture in SiB2 rapidly decreases from the beginning and then becomes stable until rainfall occurred; soil dries up slightly faster in Noah than observed; the liquid water content in CoLM looks too variable when soil freezing and thawing occurred.

In summary, three major modeling deficiencies are found: (1) at the alpine meadows, soil moisture in the topsoil is much under-predicted; (2) at the alpine deserts, soil moisture within dry soils is not well simulated; (3) at all sites, surface skin temperature for dry conditions is much under-predicted in the daytime.

4 Analyses of land processes and modeling

In this section, we present analyses of physical processes and modeling issues that are associated with the above-mentioned model deficiencies.

4.1 Soil stratification beneath alpine meadows

During the wet season, the amount of precipitation in CE-TP is usually more than 300 mm and grassroots develop well. The decomposition of the biomass in the soil is slow due to low temperature over the Plateau, and therefore, the topsoil in the CE-TP region accumulates much denser grassroots and more soil organic matters (SOM) (not shown) than the deep soil does. Table 2 shows the soil texture and parameters obtained from a laboratory soil experiment. It is clear that the topsoil has much lower

Tibet land modeling

K. Yang et al.

Title Page

Abstract

Introduction

Conclusions

References

Tables

Figures

◀

▶

◀

▶

Back

Close

Full Screen / Esc

Printer-friendly Version

Interactive Discussion



bulk density and higher soil porosity than the deep soil.

Due to this soil stratification, soil moisture observed in this region exhibits an abnormal profile. That is, soil water content is high in the topsoil and low in the deep soil, as shown in Fig. 6a–d for CE-TP sites. Such a phenomenon is not found in the western Plateau, as shown in Fig. 6e–f. Therefore, the soil stratification is related to the special climate in CE-TP.

According to an inverse analysis (Yang et al., 2005), the topsoil has high porosity and thus high water-holding capacity; this may enhance the evaporation in the wet season. On the other hand, this layer shows low heat capacity and low thermal conductivity in the dry season, which leads to high surface temperature and high sensible heat flux. With the consideration of stratified soil parameters, the soil moisture profile can be simulated well. Figure 7 shows examples at Anduo and Naqu sites, which shows near-surface soil moisture were simulated well by a LSM developed in Yang et al. (2005) with a sandwich structure to delineate the soil stratification.

There have already been some studies to formulate the effect of SOM on soil parameters (Beringer et al., 2001; Lawrence and Slater, 2008). However, laboratory soil experiments are required to measure basic parameters such as the content of grass-roots and SOM for the Plateau soils.

4.2 Soil water flow and evaporation from dry soils

Soil surface resistance (r_{soil}) is a key parameter to calculate the surface evaporation and the soil moisture within the topsoil. There are quite a few parameterizations to this resistance, as summarized in Schelde (1996), e.g., $r_{\text{soil}}=10 \exp[35.63(0.15-\theta)]$ in van de Grind and Owe (1994), $r_{\text{soil}}=3.5(\theta_{\text{sat}}/\theta)^{2.3}+33.5$ in Sun (1982), $r_{\text{soil}}=4140(\theta_{\text{sat}}-\theta)-805$ in Camillo and Gurney (1986), and $r_{\text{soil}}=\exp[8.206-4.225(\theta/\theta_{\text{sat}})]$ in Sellers et al. (1996).

Figure 8 shows the variations of r_{soil} with respect to soil water content in these parameterizations. The big difference among these parameterizations indicates that it is extremely difficult to estimate this resistance. This resistance may depend on soil mois-

Title Page

Abstract

Introduction

Conclusions

References

Tables

Figures

◀

▶

◀

▶

Back

Close

Full Screen / Esc

Printer-friendly Version

Interactive Discussion



ture, soil types, and perhaps many other factors. A new parameterization is presented below.

The continuity condition of water supply from the soil and water demand by the air must be satisfied, which may be expressed as:

$$5 \quad E = \min(\rho_w q_{\text{supply}}, E_{\text{demand}}), \quad (1)$$

$$q_{\text{supply}} = K - K \frac{\partial \psi}{\partial z}, \quad (2)$$

$$E_{\text{demand}} = \rho \frac{r h_{\text{eq}} q_{\text{sat}}(T_g) - q_a}{(r_{\text{ah}} + r_{\text{soil}})}, \quad (3)$$

where $K(\text{m s}^{-1})$ is the soil water hydraulic conductivity, and $\psi(\text{m})$ is the soil water potential. $q_{\text{supply}}(\text{m s}^{-1})$ is the maximum soil water flux from the first computational node to a very dry surface (defined by soil water potential $\psi = -10^4 \text{m}$) on the surface. E_{demand} (mm s^{-1}) is the demand water flux by the air. $r h_{\text{eq}}$ is the equilibrium relative humidity in the air space of the soil, $q_{\text{sat}}(T_g)$ is the saturated specific humidity, q_a is the air specific humidity at a reference level, and r_{ah} is the heat transfer resistance. $\rho_w(\text{kg m}^{-3})$ is the density of water, $z(\text{m})$ is the depth from the soil surface.

15 After arrangement of Eqs. (1–3), one gets

$$r_{\text{soil}} = \max \left(0, \rho \frac{r h_{\text{eq}} q_{\text{sat}}(T_g) - q_a}{\rho_w q_{\text{supply}}} - r_{\text{ah}} \right). \quad (4)$$

A key issue is how to calculate water flux within dry soils. The direct discretization to Eq. (2) would lead to unrealistic fluxes for dry soils, as soil water potential ($\psi(\theta)$) and hydraulic conductivity ($K(\theta)$) dramatically change with respect to soil moisture and the term of $K(\theta) \frac{\partial \psi(\theta)}{\partial z}$ then becomes very sensitive to the estimate of $K(\theta)$ at the interface of two adjacent computational nodes. Here, we introduce a new scheme in Ross (2003)

Title Page

Abstract

Introduction

Conclusions

References

Tables

Figures

◀

▶

◀

▶

Back

Close

Full Screen / Esc

Printer-friendly Version

Interactive Discussion



into SiB2 to investigate the importance of a computational scheme for soil water flow. Ross (2003) presented a new flux scheme based on Kirchhoff transform:

$$\phi(\theta) = \int_{-\infty}^{\psi(\theta)} K(\bar{\psi}) d\bar{\psi}, \quad (5)$$

where $\phi(\theta)$ is the so-called soil flux potential.

5 $\phi(\theta)$ has a simple form given hydraulic functions by Clapp and Hornberger (1978). Then, the soil water flow is calculated by:

$$q = K(\theta) - \frac{\partial \phi(\theta)}{\partial z}, \quad (6)$$

This transform reduces the uncertainties of calculating soil water flux as $K(\theta)$ and $\psi(\theta)$ in the second term on the RHS of Eq. (2) are merged into one term $\phi(\theta)$ in Eq. (6).

10 Another factor that may give rise to unrealistic water fluxes is the determination of the gravity flow $K(\theta)$, which is a weighted average of soil hydraulic conductivities at two nodes:

$$K(\theta) = wK_1 + (1 - w)K_2. \quad (7)$$

Ross (2003) proposed a dynamic estimation to the weight number:

$$15 \quad w = \left(\frac{\phi(\psi_2 - \Delta z) - \phi(\psi_2)}{\Delta z} + K_2 \right) / (K_2 - K(\psi_2 - \Delta z)). \quad (8)$$

where subscripts 1 and 2 denotes two adjacent nodes and Δz the distance between the nodes.

20 As indicated in Fig. 9, after introducing the above-mentioned Ross scheme and the new parameterization of soil surface resistance into SiB2, the simulated soil moisture in top 15 cm is closer to the observed one.

Title Page

Abstract

Introduction

Conclusions

References

Tables

Figures

◀

▶

◀

▶

Back

Close

Full Screen / Esc

Printer-friendly Version

Interactive Discussion



4.3 Heat flux parameterization

As shown in Figs. 3b and 5a, the peak of the daytime surface temperature is significantly under-predicted for dry surfaces. This is a common issue for land surface modeling in arid and semiarid regions, as shown in Yang et al. (2007).

5 According to Yang et al. (2008), an excess resistance must be introduced to estimate sensible heat flux from ground and air temperature difference. This resistance is due to the difference between the aerodynamic roughness length and the thermal roughness length. There are a number of studies on the parameterization of the resistance. Yang et al. (2008) presented the latest progress in this topic. Their study indicates that the
10 thermal roughness length depends on flow state and exhibits diurnal variations. Similar findings are also found in other sites (e.g., Sun, 1999; Liu et al., 2007). In particular, ground-air temperature differences in the Plateau region can exceed 30 K, and the diurnal variations of the thermal roughness length are more evident than in other regions. However, many models neglect the difference between the two roughness lengths or specify a constant value of their ratio (typically 7.3 or 10). Noah model uses Zilitinkevich (1995) scheme to calculate the roughness length, and Yang et al. (2008) pointed
15 out that this scheme may over-estimate the roughness length and thus underestimate peak values of the surface temperature.

Figure 10 shows the results of SiB2 with and without accounting for the excess resistance which is recommended in Yang et al. (2008). It is shown that the ground-air temperature difference is well simulated by SiB2 when the excess resistance is included in the modeling, while the simulation without the excess resistance actually yields higher sensible heat fluxes though its surface temperature is under-estimated. This can be
20 explained as follows.

25 For a dry surface, the evaporation is neglected. When the surface temperature is under-estimated, the net radiation would be over-estimated, and thus, the sensible heat flux would be over-predicted, and vice versa. The results in Fig. 10 exactly verify this reasoning. Undoubtedly, the parameterization to the excess resistance or the thermal

Title Page

Abstract

Introduction

Conclusions

References

Tables

Figures



Back

Close

Full Screen / Esc

Printer-friendly Version

Interactive Discussion



roughness length is very crucial for reproducing the surface temperature and sensible heat flux simultaneously.

5 Conclusions and recommendations

The Tibetan Plateau is a key region of land-atmosphere interactions. This study evaluated the performance of three state-of-the-art land surface models (SiB2, Noah, CoLM) in the Plateau region. Major findings are as follows.

First, water content within the topsoil of CE-TP alpine meadows is commonly under-predicted by all models, due to the soil stratification. The soil stratification issue was also investigated by van der Velde et al. (2009). The topsoil beneath the meadows contains dense grassroots and affluent soil organic matters. Limited experiments have shown this layer exhibits properties different from the deep soil (e.g. higher soil porosity, low bulk density), and in general, high soil water content was observed in the topsoil. This special while widely occupied land type has not been taken into account in current models. Certainly, more soil hydraulic and thermal experiments are crucial for developing a parameterization scheme for the soil stratification.

Second, it is shown that the modeling of soil water content within dry soils can be improved with an appropriate parameterization of soil surface resistance for evaporation and an advanced scheme for soil water flux.

Third, daytime ground-air temperature gradient for the western alpine deserts is under-predicted. This under-estimation actually corresponds to the overestimate of sensible heat flux, and all these errors result from the under-estimation (or neglect) of an excess resistance for heat transfer. In recent decades, it has been recognized that the thermal roughness length differs from the aerodynamic transfer resistance, and therefore an excess resistance is required for calculating heat transfer. However, this crucial issue is not well solved in current models (e.g., a fixed ratio of the aerodynamic roughness length to the thermal roughness length is given) and it causes surface temperature being underestimated by 10 K for the alpine desert or net radia-

Tibet land modeling

K. Yang et al.

Title Page

Abstract

Introduction

Conclusions

References

Tables

Figures

◀

▶

◀

▶

Back

Close

Full Screen / Esc

Printer-friendly Version

Interactive Discussion



tion being over-estimated by 40 W m^{-2} or so. This study integrates into SiB2 a diurnally variable thermal roughness length recommended in Yang et al. (2008), and it is shown the ground-air temperature gradient over very dry surfaces can be simulated well. This scheme can also be extended to other arid and semi-arid regions.

Therefore, in addition to the well-known snow melting and soil freezing/thawing processes, there are some special while dominant processes in the Plateau. In order to simulate well the Plateau surface water and energy budget, future activities should pursue both field and laboratory experiments for appropriately representing these processes in land surface models. Process studies on the dissimilarity between the Plateau and lowland areas and the similarity between the Plateau and the Polar regions may also provide new clues for improving our understanding and modeling of the Plateau land processes.

Acknowledgements. This work was supported by NSFC grants (Grant Number 40875009) and by the CAS “Hundred Talent” Project. The in situ data used in this paper were obtained under the GAME/Tibet project, which was supported by the MEXT, FRSGC, NASDA of Japan, Chinese Academy of Science, and Asian Pacific Network. The NWP MOLTS data were provided by the CEOP Centralized Data Archive System.

References

- Beringer, J., Lynch, A. H., Chapin III, F. S., Mack, M., and Bonan, G. B.: The Representation of Arctic Soils in the Land Surface Model: The Importance of Mosses, *J. Climate*, 14, 3321–3335, 2001.
- Camillo, P. J. and Gurney, R. J.: A resistance parameter for bare soil evaporation models, *Soil Sci.*, 141, 95–105, 1986.
- Chen, F., Mitchell, K., Schaake, J., Xue, Y., Pan, H.-L., Koren V., Duan, Q.-Y., Ek, M., and Betts A., 1996: Modeling of land-surface evaporation by four schemes and comparison with FIFE observations, *J. Geophys. Res.*, 101(D3), 7251–7268.
- Clapp, R. B. and Hornberger, G. M.: Empirical Equations for Some Soil Hydraulic Properties, *Water Resour. Res.*, 14(4), 601–604, 1978.

Tibet land modeling

K. Yang et al.

Title Page

Abstract

Introduction

Conclusions

References

Tables

Figures



Back

Close

Full Screen / Esc

Printer-friendly Version

Interactive Discussion



Tibet land modeling

K. Yang et al.

Dai, Y.-J., Zeng, X.-B., Dickinson, R. E., Baker, I., Bonan, G. B., Bosilovich, M. G., Denning, A. S., Dirmeyer, P. A., Houser, P. R., Niu, G.-Y., Oleson, K. W., Schlosser, C. A., and Yang, Z.-L.: The Common Land Model (CLM), *B. Amer. Meteor. Soc.*, 84, 1013–1023, 2003.

Global Soil Data Task: Global Gridded Surfaces of Selected Soil Characteristics (IGBPDIS), International Geosphere-Biosphere Programme – Data and Information Services, available online at: <http://www.daac.ornl.gov/> (last access: February 2003) from the ORNL Distributed Active Archive Center, Oak Ridge National Laboratory, Oak Ridge, Tennessee, USA, 2000.

Hansen, M. C., DeFries, R. S., Townshend, J. R. G., and Sholberg, R.: Global land cover classification at 1 km spatial resolution using a classification tree approach, *Int. J. Remote Sens.*, 21, 1331–1364, 2000.

Hu, H.-P., Ye, B.-S., Zhou, Y.-H., and Tian, F.-Q.: A land surface model incorporated with soil freeze/thaw and its application in GAME/Tibet, *Sci. China Ser. D*, 49(12), 1311–1322, 2006.

Koike, T.: The Coordinated Enhanced Observing Period – an initial step for integrated global water cycle observation, *WMO Bulletin*, 53(2), 1–8, 2004.

Koike, T., Yasunari, T., Wang, J., and Yao, T.: GAME-Tibet IOP summary report, in: *Proceeding of the 1st International Workshop on GAME-Tibet*, Xi'an, China, 11–13 January 1999, 1–2, 1999.

Koren, V., Schaake, J., Mitchell, K., Duan, Q.-Y., Chen, F., and Baker, J. M.: A parameterization of snowpack and frozen ground intended for NCEP weather and climate models, *J. Geophys. Res.*, 104, 19569–19585, 1999.

Lawrence, D. M. and Slater, A. G.: Incorporating organic soil into a global climate model, *Clim. Dyn.*, 30, 145–160, doi:10.1007/s0038200702781, 2008.

Li, Q. and Sun, S.-F.: Development of the universal and simplified soil model coupling heat and water transport, *Sci. China Ser.-D*, 51, 88–102, 2008.

Liu, S.-M., Lu, L., Mao, D., and Jia, L.: Evaluating parameterizations of aerodynamic resistance to heat transfer using field measurements, *Hydrol. Earth Syst. Sci.*, 11, 769–783, 2007, <http://www.hydrol-earth-syst-sci.net/11/769/2007/>.

Loveland, T. R., Reed, B. C., Brown, J. F., Ohlen, D. O., Zhu, Z., Yang, L. and Merchant, J. W.: Development of a global land cover characteristics database and IGBP DISCover from 1-km AVHRR data. *Int. J. Remote Sens.*, 21, 1303–1330, 2001.

Ma, Y.-M., Tsukamoto, O., Wang J., Ishikawa, H., and Tamagawa, I.: Analysis of aerodynamic and thermodynamic parameters over the grassy marshland surface of Tibetan Plateau, *Prog. Nat. Sci.*, 12, 36–40, 2002.

Title Page

Abstract

Introduction

Conclusions

References

Tables

Figures

◀

▶

◀

▶

Back

Close

Full Screen / Esc

Printer-friendly Version

Interactive Discussion



- Ma, Y.-M., Kang, S.-C., Zhu, L.-P., Xu, B.-Q., Tian, L.-D. and Yao, T.-D.: Tibetan Observation And Research Platform (Torp): Atmosphere-Land Interaction Over A Heterogeneous Landscape, *B. Amer. Meteor. Soc.*, 89, 1487–1492, 2008.
- Nemoto, T., Koike, T., and Kitsuregawa, M.: Data Analysis System Attached to the CEOP Centralized Data Archive System, *J. Meteorol. Soc. Jpn.*, 85A, 529–543, 2007.
- Ross, P. J.: Modeling soil water and solute transport – Fast, simplified numerical solutions, *Agron. J.*, 95, 1352–1361, 2003.
- Schelde, K.: Modelling the Forest Energy and Water Balance, Series Paper No. 62, Department of Hydrodynamics and Water Resources Technical University of Denmark, 2800 Lyngby, Danmark, 263 pp., 1996
- Sellers, P. J., Randall, D. A., Collatz, G. J., Berry, J. A., Field, C. B., Dazlich, D. A., Zhang, C., Collelo, G. D., and Bounoua, L.: A revised land surface parameterization (SiB2) for atmospheric GCMs. Part I: Model formulation, *J. Climate*, 9, 676–705, 1996.
- Sun, J.: Diurnal variations of thermal roughness height over a grassland. *Bound-Lay. Meteorol.*, 92, 404–427, 1999.
- Sun, S.-F.: Moisture and heat transport in a soil layer forced by atmospheric conditions. M.S. thesis, Dept. of Civil Engineering, University of Connecticut, 72 pp, 1982.
- Takayabu, I., Takata, K., Yamazaki, T., Ueno, K., Yabuki, H., and Haginoya, S.: Comparison of the Four Land Surface Models Driven by a Common Forcing Data Prepared from GAME/Tibet POP'97 Products – Snow Accumulation and Soil Freezing Processes, *J. Meteorol. Soc. Jpn.*, 79(1B), 535–554, 2001.
- Tanaka, K., Tamagawa, I., Ishikawa, H., Ma, Y.-M. and Hu, Z.: Surface energy and closure of the eastern Tibetan Plateau during the GAME-Tibet IOP 1998, *J. Hydro.*, 283, 169-183, 2003.
- van de Grind, A. A. and Owe, M.: Bare soil surface resistance to evaporation by vapor diffusion under semiarid, *Water Resour. Res.*, 30, 181–188, 1994.
- van der Velde, R., Su, Z., Ek, M., Rodell, M., and Ma, Y.: Influence of thermodynamic soil and vegetation parameterizations on the simulation of soil temperature states and surface fluxes by the Noah LSm over a Tibetan plateau site, *Hydrol. Earth Syst. Sci. Discuss.*, 6, 455–499, 2009,
<http://www.hydrol-earth-syst-sci-discuss.net/6/455/2009/>.
- Watanabe, T. and Kondo, J.: The influence of canopy structure and density upon the mixing length within and above vegetation, *J. Meteorol. Soc. Jpn.*, 68, 227–235, 1990.

Tibet land modeling

K. Yang et al.

Title Page

Abstract

Introduction

Conclusions

References

Tables

Figures

◀

▶

◀

▶

Back

Close

Full Screen / Esc

Printer-friendly Version

Interactive Discussion



Tibet land modeling

K. Yang et al.

- Xu, X.-D., Zhou, M.-Y., Chen, J.-Y., Bian, L.-G., Zhang, G.-Z., Liu, H.-Z., Li, S.-M., Zhang, H.-S., Zhao, Y.-J., Suolongduoji, and Wang J.-Z.: A comprehensive physical pattern of land-air dynamic and thermal structure on the Qinghai-Xizang Plateau, *Sci. China Ser. D*, 45, 577–595, 2002.
- 5 Xu, X.-D., Zhang, R.-H., Koike, T., Lu, C.-G., Shi, X.-H., Zhang, S.-J., Bian, L.-G., Cheng, X.-H., Li, P.-Y., and Ding, G.-A.: A New Integrated Observational System over the Tibetan Plateau (NIOST), *B. Am. Meteor. Soc.*, 89(10), 1492–1496, 2008.
- Yanai, M., Li, C. and Song, Z.: Seasonal heating of the Tibetan Plateau and its effects on the evolution of the Asian summer monsoon, *J. Meteorol. Soc. Jpn.*, 70, 319–351, 1992.
- 10 Yanai, M. and Wu, G.-X.: Effect of the Tibetan Plateau, *The Asian Monsoon*, edited by: Wang, B., Springer, 513–549, 2006.
- Yang, K., Koike, T., Ishikawa, H., and Ma, Y.-M.: Analysis of the Surface Energy Budget at a site of GAME/Tibet using a Single-Source Model, *J. Meteorol. Soc. Jpn.*, 82, 131–153, 2004.
- Yang, K., Koike, T., Ye, B.-S., and Bastidas, L.: Inverse analysis of the role of soil vertical heterogeneity in controlling surface soil state and energy partition, *J. Geophys. Res.*, 110, D08101, doi:10.1029/2004JD005500, 2005.
- 15 Yang, K., Rasmy, M., Rauniyar, S., Koike, T., Taniguchi, K., Tamagawa, K., Koudelova, P., Kitsuregawa, M., Nemoto, T., Yasukawa, M., Ikoma, E., Bosilovich, M., and Williams, S.: Initial CEOP-based review of the prediction skill of operational general circulation models and land surface models, *J. Meteorol. Soc. Jpn.*, 85A, 99–116, 2007.
- 20 Yang, K., Koike, T., Ishikawa, H., Kim, J., Li, X., Liu, H.-Z., Liu, S.-M., Ma, Y.-M., Wang, J.-M.: Turbulent flux transfer over bare soil surfaces: Characteristics and parameterization, *J. Appl. Meteorol. Clim.*, 40, 276–290, 2008.
- 25 Ye, D.-Z. and Gao, Y.: *The Meteorology of the Qinghai-Xizang (Tibet) Plateau* (in Chinese), Beijing, Science Press, 278 pp., 1979.

Title Page

Abstract

Introduction

Conclusions

References

Tables

Figures

◀

▶

◀

▶

Back

Close

Full Screen / Esc

Printer-friendly Version

Interactive Discussion



Tibet land modeling

K. Yang et al.

Table 1. The model structure of SiB2, Noah, and CoLM.

	SiB2	Noah	CoLM
Number of soil layers	3	4	10
Temperature solver	force restore	thermal diffusion equation	thermal diffusion equation
Soil surface evaporation resistance	Yes	Accounted indirectly	No
Soil stratification	No	No	Yes
Soil freezing and thawing	No	Yes	Yes
Soil parameters	ISLSCP-II	FAO	FAO+STATSGO
Land use parameters	ISLSCP-II	UMD Vegetation classification map	USGS

Title Page

Abstract

Introduction

Conclusions

References

Tables

Figures

◀

▶

◀

▶

Back

Close

Full Screen / Esc

Printer-friendly Version

Interactive Discussion



Table 2. Soil composition and parameters analyzed by laboratory experiments for Anduo site for five field samples (two at 5 cm, two at 20 cm, and one at 60 cm) (courtesy of N. Hirose).

Sample No.	Depth (cm)	Sample features	Composition (%)				ρ_d (kg m^{-3})	θ_s ($\text{m}^3 \text{m}^{-3}$)
			Gravel	Sand	silt	clay		
5A	5	dense root			N/A		0.667	0.633
5B	5	dense root	0.00	30.64	59.88	9.48	0.817	0.593
20A	20	little root, gravel	3.69	69.02	19.83	7.46	1.378	0.440
20B	20	little root, gravel	4.24	67.08	19.53	9.15	1.694	0.318
60	60	little root, gravel	3.35	76.56	10.12	9.97	1.426	0.370

Title Page

Abstract

Introduction

Conclusions

References

Tables

Figures



Back

Close

Full Screen / Esc

Printer-friendly Version

Interactive Discussion



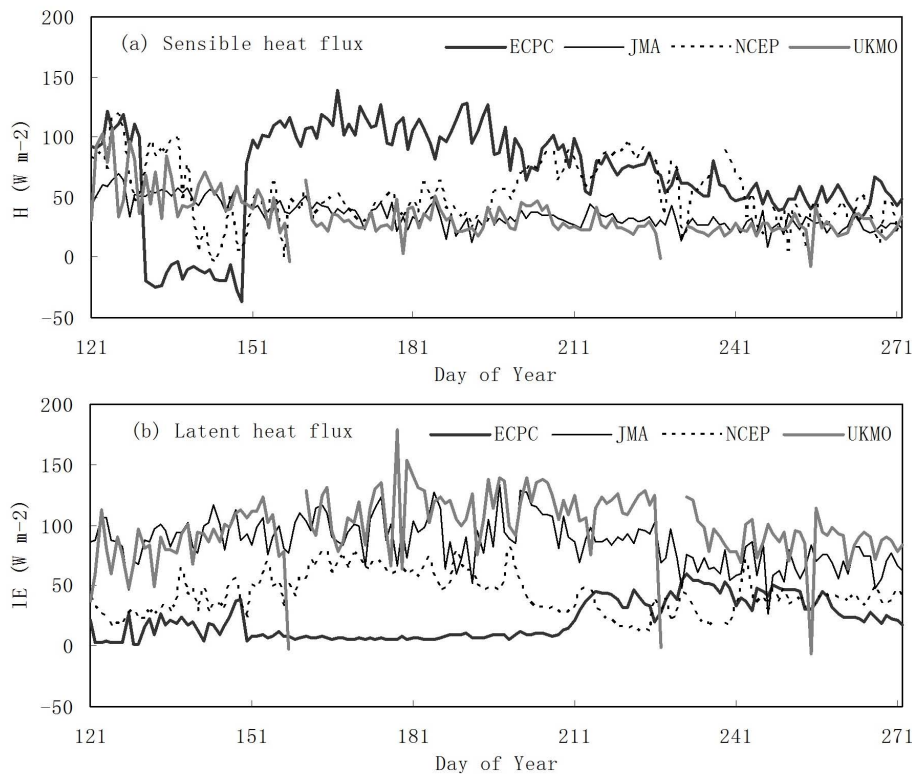


Fig. 1. Seasonal march of daily surface energy budget in four numerical weather prediction models for the CEOP eastern Tibet site (31.379° N, 91.9° E, 4580 m a.s.l.), 2003.

Title Page

Abstract

Introduction

Conclusions

References

Tables

Figures

◀

▶

◀

▶

Back

Close

Full Screen / Esc

Printer-friendly Version

Interactive Discussion



Tibet land modeling

K. Yang et al.

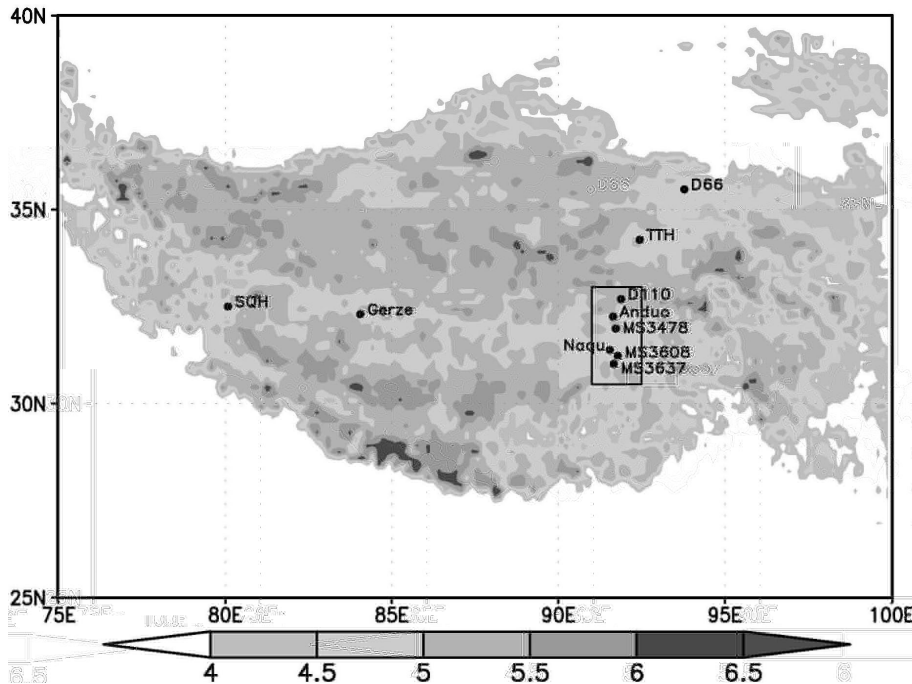


Fig. 2. Map of GAME-Tibet Experiment, IOP 1998. Grey bar represents elevation in km. The small rectangle is the mesoscale experimental area (91–92.5° E, 30.5–33° N). SQH and TTH are the abbreviation of Shiquanhe and Tuotuohe sites of GAME-Tibet experiments, respectively.

Title Page

Abstract

Introduction

Conclusions

References

Tables

Figures

◀

▶

◀

▶

Back

Close

Full Screen / Esc

Printer-friendly Version

Interactive Discussion



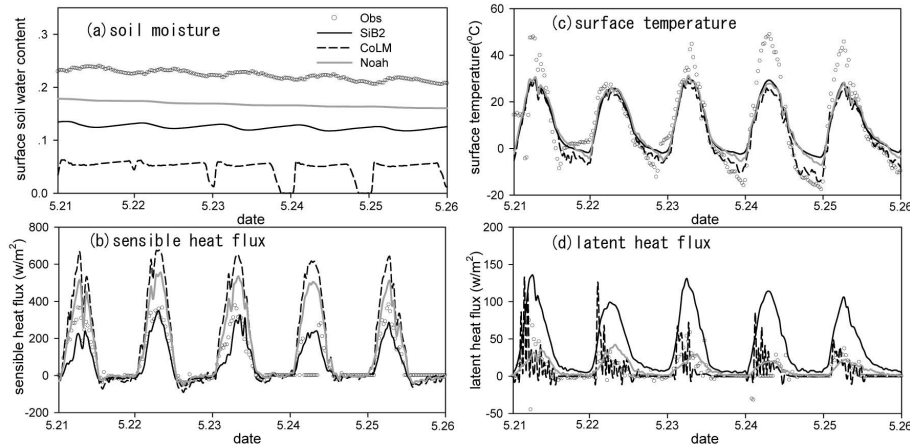


Fig. 3. Simulated near-surface soil moisture, surface skin temperature, sensible heat flux, and latent heat flux at an alpine meadow site (Anduo) for the pre-monsoon season, 1998.

Title Page

Abstract

Introduction

Conclusions

References

Tables

Figures

◀

▶

◀

▶

Back

Close

Full Screen / Esc

Printer-friendly Version

Interactive Discussion



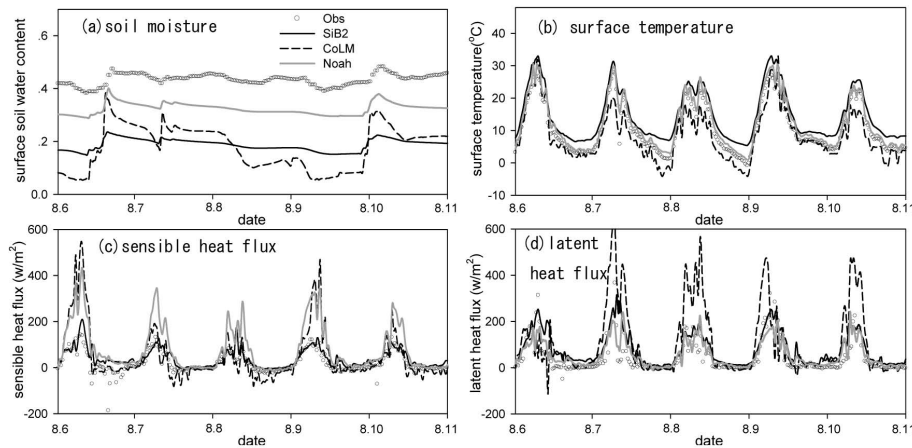


Fig. 4. Similar to Fig. 3, but for the monsoon season.

Title Page

Abstract

Introduction

Conclusions

References

Tables

Figures

◀

▶

◀

▶

Back

Close

Full Screen / Esc

Printer-friendly Version

Interactive Discussion



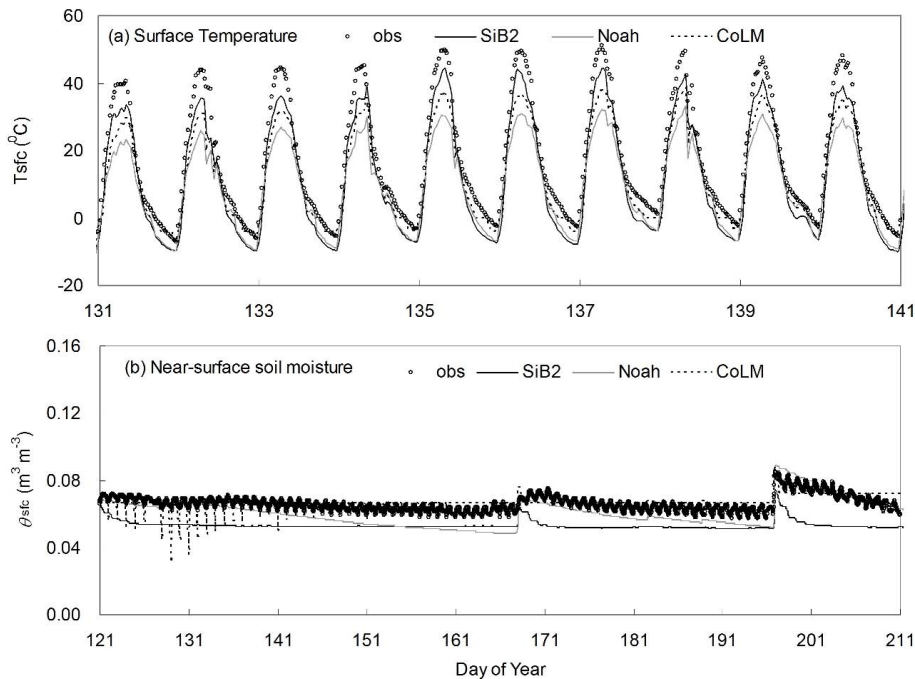


Fig. 5. Simulated near-surface soil moisture and surface skin temperature at an alpine desert site (SQH), 1998. Panel (a) only shows the simulation of a selected period.

Title Page

Abstract

Introduction

Conclusions

References

Tables

Figures

◀

▶

◀

▶

Back

Close

Full Screen / Esc

Printer-friendly Version

Interactive Discussion



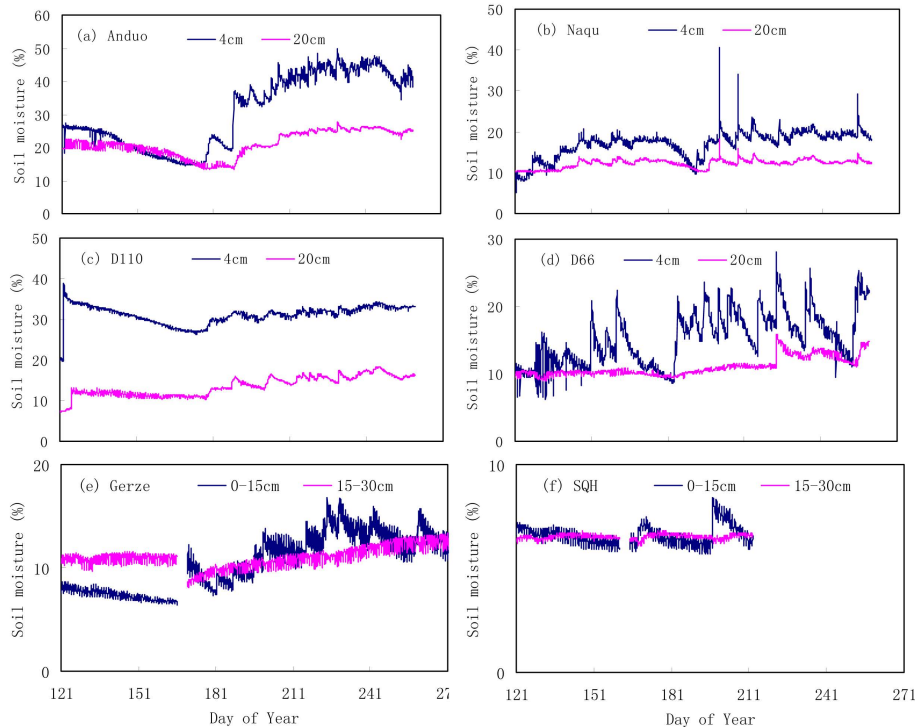


Fig. 6. Observed soil water content in the near-surface soil and the deeper soil at GAME-Tibet sites, 1998 (Soil moisture at Naqu was not measured in 1998; plotted is the data for 2001). Panels (a–d) for CE-TP alpine meadow sites and panels (e–f) for W-TP sites.

Title Page

Abstract

Introduction

Conclusions

References

Tables

Figures

◀

▶

◀

▶

Back

Close

Full Screen / Esc

Printer-friendly Version

Interactive Discussion



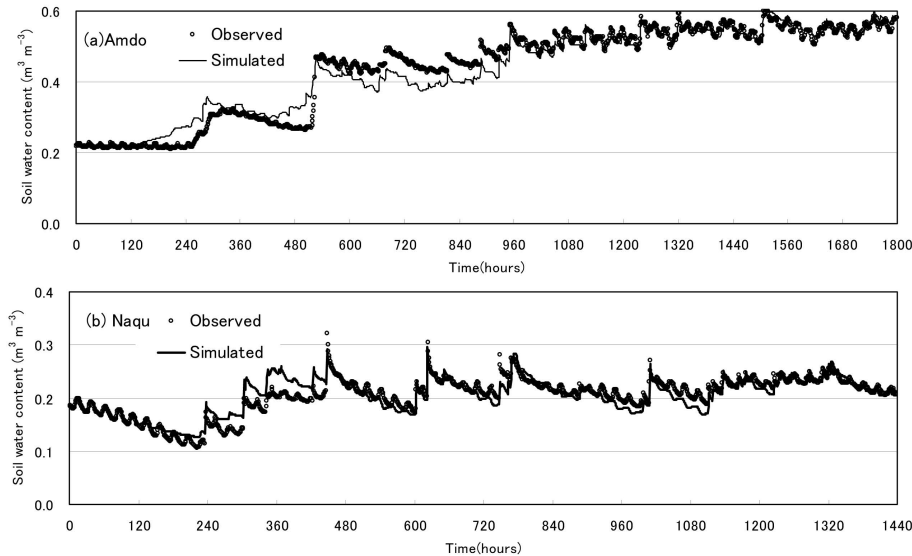


Fig. 7. Comparisons of near-surface soil water content between observation and simulation at Anduo site in 1998 and Naqu site in 2001. The simulations were conducted using the LSM in Yang et al. (2005) with stratified soil parameters.

Title Page

Abstract

Introduction

Conclusions

References

Tables

Figures

◀

▶

◀

▶

Back

Close

Full Screen / Esc

Printer-friendly Version

Interactive Discussion



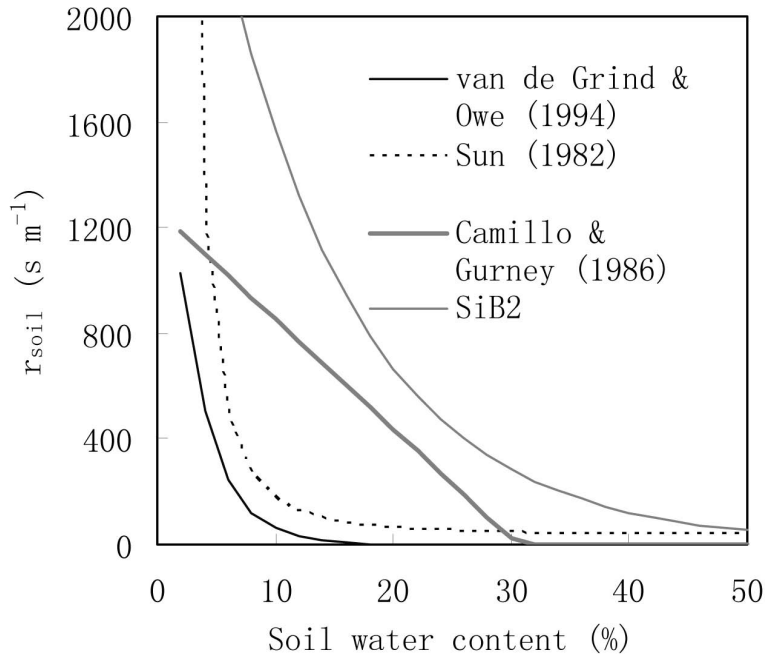


Fig. 8. Comparisons of formulas of soil surface resistance for evaporation (see the formulas in the text).

Title Page

Abstract

Introduction

Conclusions

References

Tables

Figures

◀

▶

◀

▶

Back

Close

Full Screen / Esc

Printer-friendly Version

Interactive Discussion



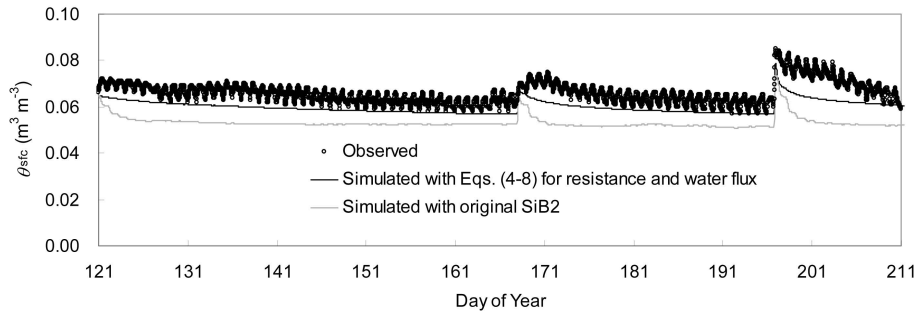


Fig. 9. Comparison of soil water content between observation and simulation at an alpine desert site (SQH). The simulation is conducted using SiB2 with or without Eqs. (4–8) for calculating soil water flow and evaporation.

Title Page	
Abstract	Introduction
Conclusions	References
Tables	Figures
◀	▶
◀	▶
Back	Close
Full Screen / Esc	
Printer-friendly Version	
Interactive Discussion	



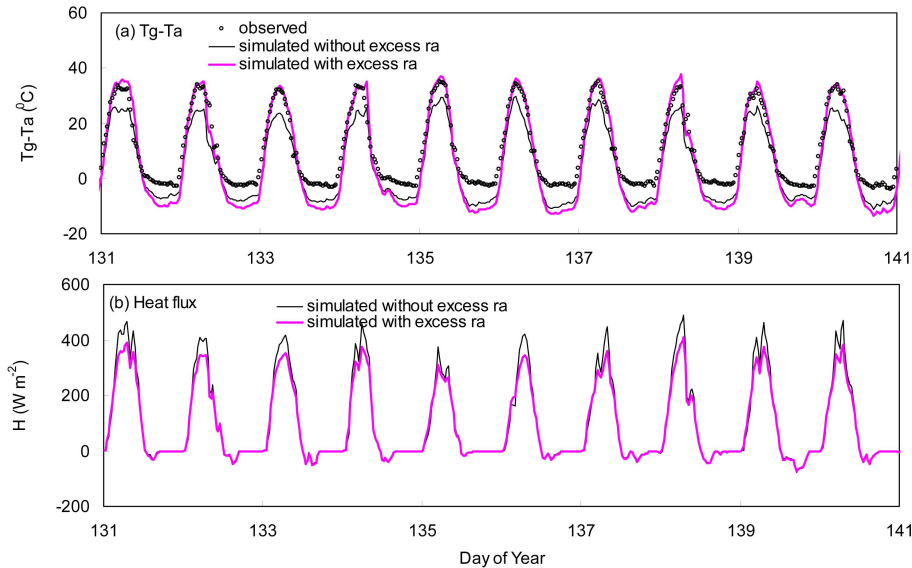


Fig. 10. Comparisons between two SiB2 simulations with and without excess heat transfer resistance for an alpine desert site (SQH) in 1998. Panel (a) ground-air temperature gradient, (b) sensible heat flux.

Title Page

Abstract

Introduction

Conclusions

References

Tables

Figures

◀

▶

◀

▶

Back

Close

Full Screen / Esc

Printer-friendly Version

Interactive Discussion

